

Figure S1. The calibration curve for the measurement of sorafenib concentrations in DMSO shows how the measured absorbance and known sorafenib concentrations relate to each other for precise dose estimation.

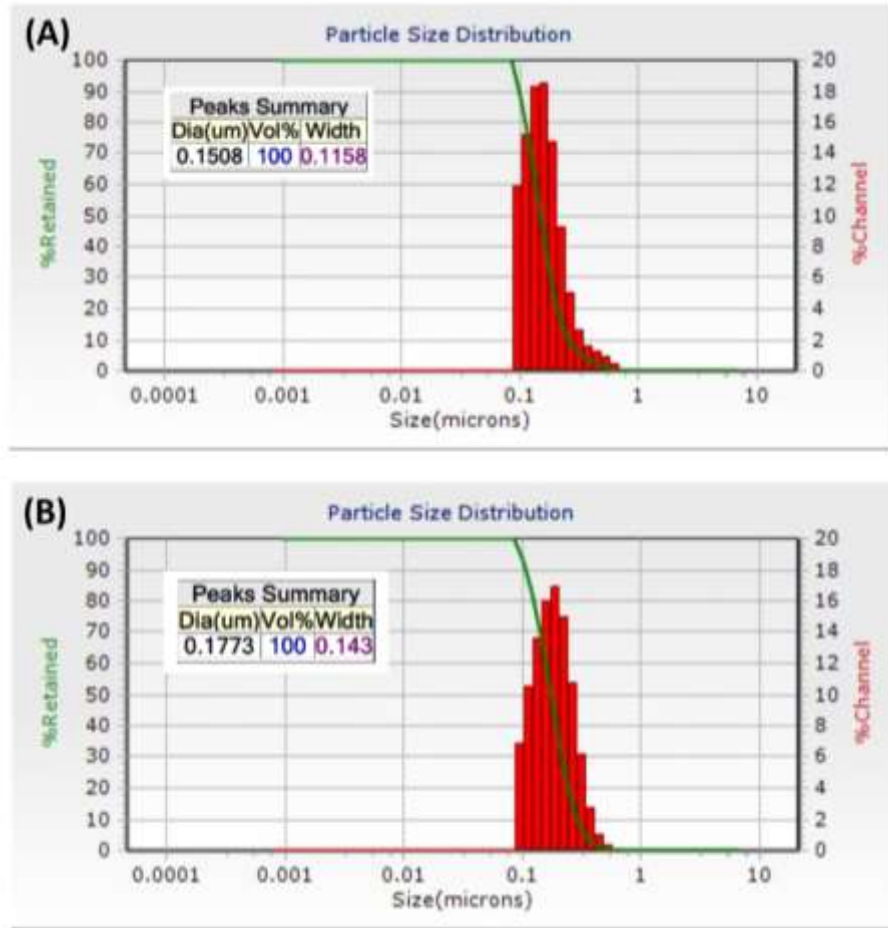


Figure S2. Dynamic light scattering (DLS) analysis of particle size distribution for various niosomal formulations. (A) sorafenib-loaded, niosomes (SOR@Nio) (B) sorafenib-loaded, hyaluronic acid-functionalized niosomes (SOR@Nio/HA). The results show an increase in particle size upon surface modification with HA, indicating successful conjugation and encapsulation. Size distribution remained within the nanometric range suitable for passive and active tumor targeting.

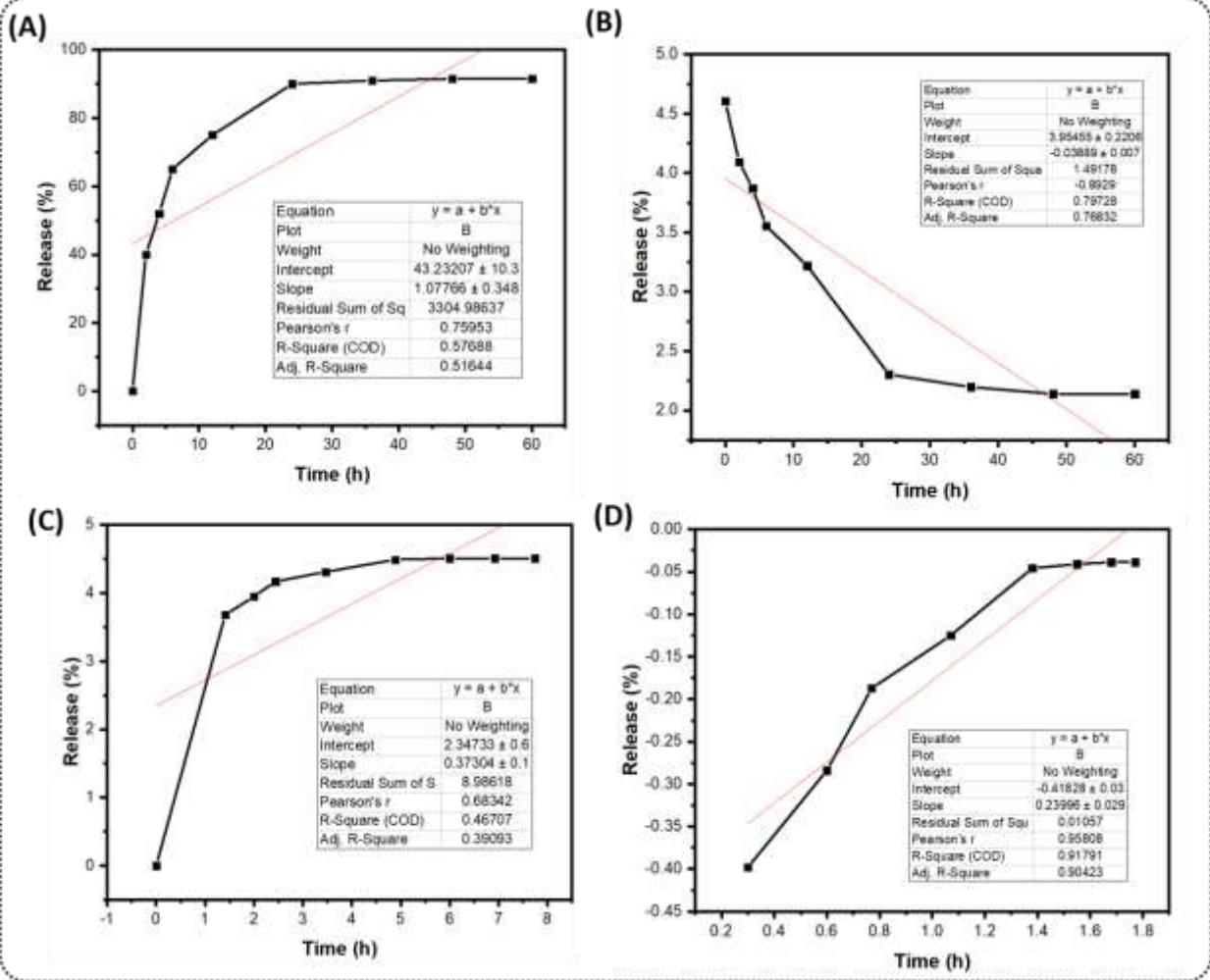


Figure S3. In vitro drug release profiles fitted to different kinetic models (A: Zero-order, B: First-order, C: Higuchi, D: Korsmeyer–Peppas). Black squares show experimental data and red lines indicate model fitting. Insets present regression equations and statistical parameters (R^2 , adjusted R^2 , Pearson's r).

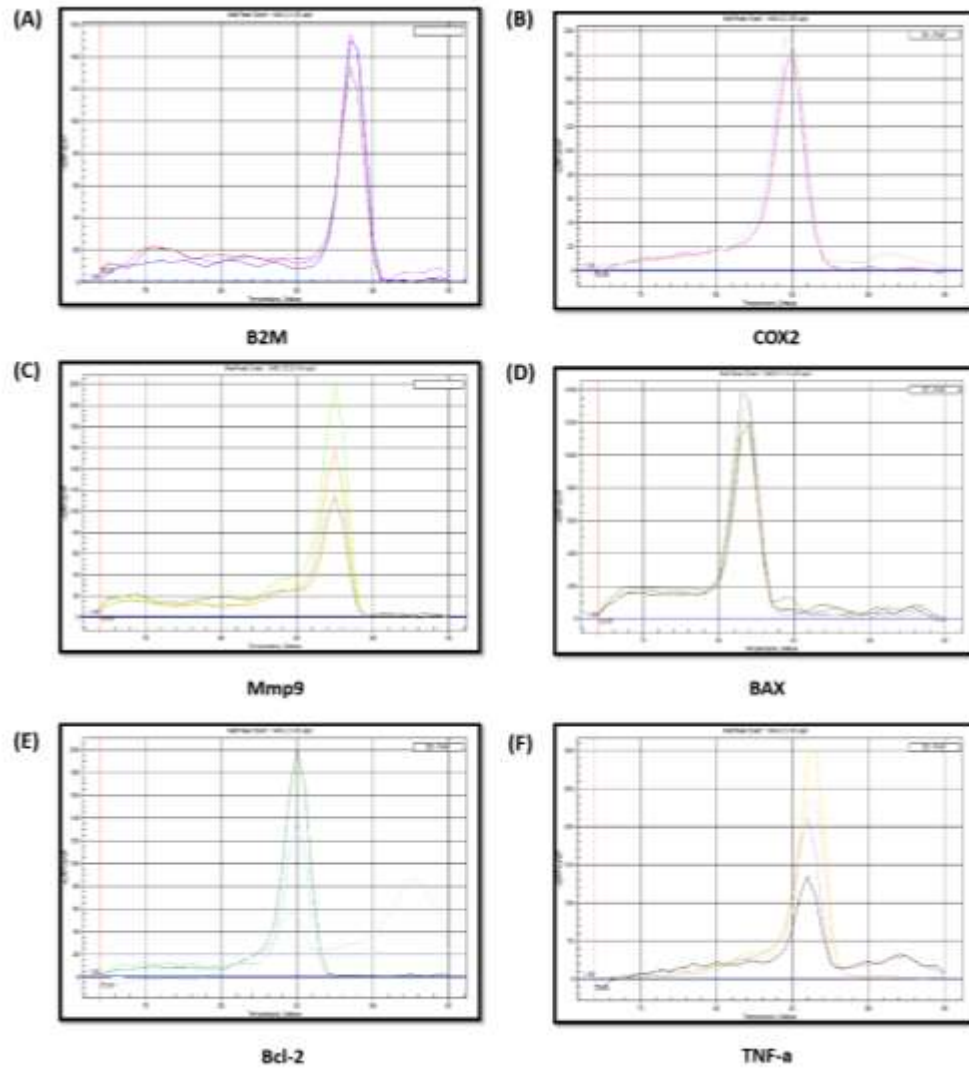


Figure S4. Melting curve analysis of qRT-PCR products confirming the specificity of amplification for each gene target. (A) B2M, (B) COX-2, (C) MMP-9, (D) BAX, (E) Bcl-2, and (F) TNF- α . The presence of single sharp peaks indicates the absence of primer-dimers and non-specific amplification, ensuring reliability of the gene expression data.

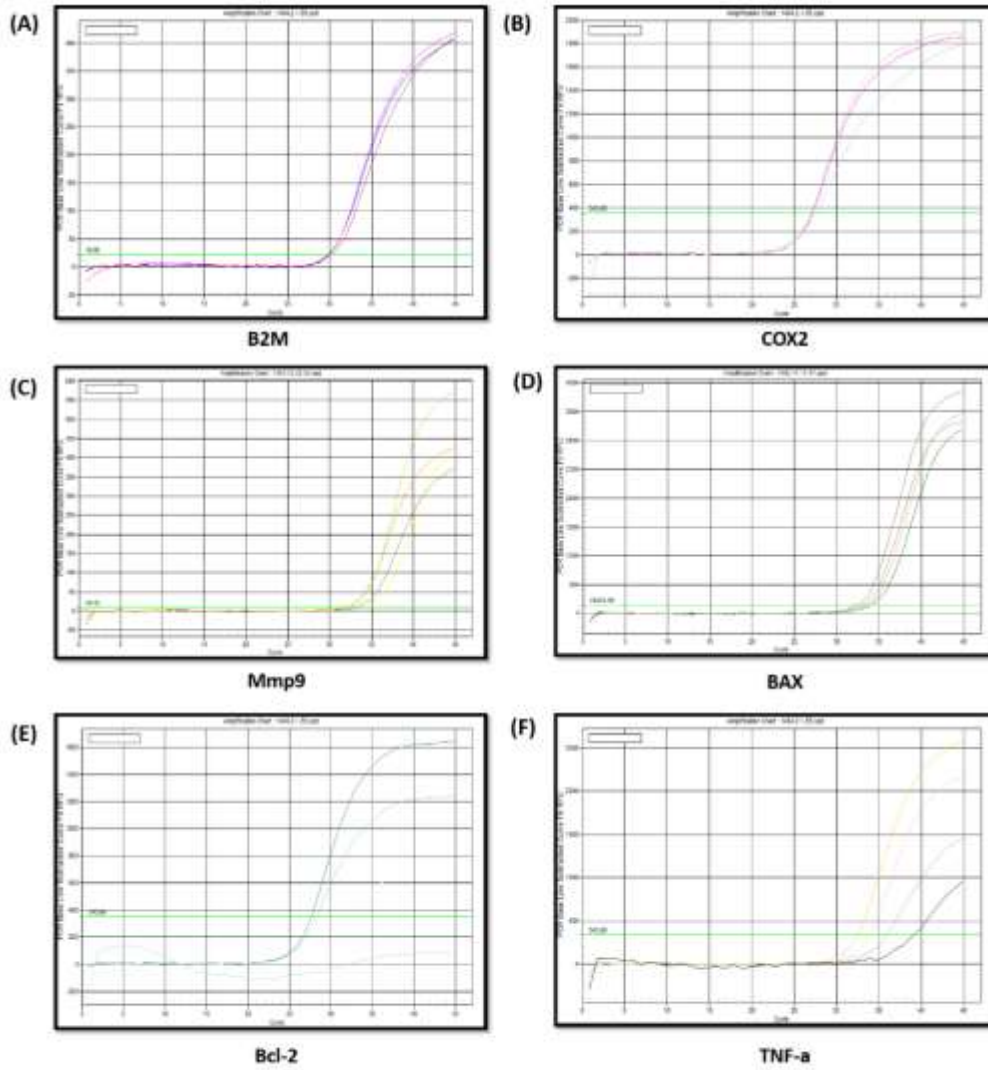


Figure S5. Quantitative real-time PCR (qRT-PCR) amplification plots for gene expression analysis in CAL27 cells treated with various formulations. (A) B2M (housekeeping gene), (B) COX-2, (C) MMP-9, (D) BAX, (E) Bcl-2, and (F) TNF- α . These plots demonstrate differential gene expression patterns in response to SOR@Nio/HA, indicating effects on inflammation, apoptosis, and metastasis-related pathways.